Biospherical Instruments Inc.

APPLICATION NOTE:

Understanding GUV Calibrations

Application Note #: AN-2015-0001-Rev1
BSI DCN 006464KA

Understanding GUV Calibrations

1. INTRODUCTION

GUV instruments are above-water multi-channel filter radiometers that measure global irradiance from Sun and sky at several wavelengths in the UV and visible. The original model of the GUV series was the GUV-511. It was introduced in 1992 and featured five channels at 305, 320, 340, and 380 nm, as well as a channel to measure Photosynthetically Active Radiation (PAR; 400–700 nm)[1]. The GUV-511 was replaced in 2003 by the GUV-2511 radiometer, which has a larger dynamic range and expanded channel selection. In 2014, the GUVis-3511 was introduced. This all-new instrument can be equipped with up to 19 spectral channels and a shadowband accessory. It is based on BSI's microradiometer technology. The new electronics feature unprecedented performance with respect to dynamic range, linearity, speed, and expandability. Detailed information on Biospherical Instrument's (BSI) line of GUV instruments (including PUV radiometers for in-water measurements) is available at http://www.biospherical.com.

The overall objective of this document is to give owners of GUV radiometers the knowledge to select the calibration method that is best suited for their application, and to describe advantages, disadvantages, and limitations of the various methods. Some calibration methods require the measurement of the GUV's "spectral response function." This (rather labor-intensive) characterization is typically not included in a typical GUV delivery but can be ordered if a user's application calls for it. A secondary objective is therefore to discuss the benefits of such a characterization. For example, the standard calibration method that is typically applied to GUV raw data may lead to significant systematic errors for low-Sun conditions. These errors can be corrected if the spectral response functions of the GUV's channels are known.

This document does not describe the instruments' hardware, the amplification and conversion of photodiode currents to signal output, and data formats. Instead, it describes calibration approaches and implementation. These methods can be applied to any of the three GUV models introduced above.

[1] As and alternative to the GUV-511, also the GUV-541 was offered , which uses a 313 nm channel instead of a PAR channel.

Section 2 provides an overview of the calibration methods that are recommended by the World Meteorological Organization and Section 3 discusses BSI's implementations of these methods. Section 4 discusses the important differences of calibrations obtained with a calibration lamp and those obtained vicariously against a scanning spectroradiometer. Section 5 describes systematic errors in calibrated solar data and their corrections. Section 6 introduces the calculation of secondary data products — such as the UV Index or UV-B irradiance — from calibrated GUV data. A description of the measurement of spectral response functions and a Glossary are provided in Appendices.

2. CALIBRATION METHODS

The calibration methods implemented by BSI are based on recommendations provided by the World Meteorological Organization (Seckmeyer et al., 2010). The following description is adopted from this reference but also takes requirements and specifications of GUV instruments into account.

There are two fundamentally different approaches of calibrating multi-channel filter instruments. The two approaches result in different radiometric quantities. The first approach is based on a comparison of GUV raw data with either the solar spectral irradiance measured by a spectroradiometer or with the spectral irradiance from a calibration standard (i.e., a 1000 Watt FEL lamp with a scale of spectral irradiance traceable to the U.S. National Institute of Standards and Technology, NIST). The second approach requires that the spectral response functions (see definition in Appendix A.3) of all channels of a GUV radiometer are accurately known. Both methods are implemented by BSI.

- **Approach 1 – Spectral Irradiance**
  The objective of Approach 1 is to establish a calibration factor for each channel of the instrument which, when applied to the GUV's raw signal, returns spectral irradiance at the nominal wavelength of the channel. For example, a "solar-based" calibration factor is defined such that the calibrated measurement of each channel approximates the spectral irradiance measured by BSI's SUV-100 spectroradiometer (Appendix A.1), which has a bandpass of 1 nm. (This example assumes that spec-

troradiometer and filter instrument are exposed to the same radiation field.)

The advantage of Approach 1 is that the result of the measurement — spectral irradiance — is a common radiometric quantity. The disadvantage is that calibration factors depend on the radiation source measured because the bandpass of GUV channels of typically 10 nm does not match that of the spectroradiometer. For example, calibration factors established with the Sun as the "light source" are different from those established with a FEL calibration lamp (Section 4). The shape of the solar spectrum also depends on the solar zenith angle (SZA) and other atmospheric parameters such as total column ozone (TOC). Solar-based calibration factors therefore also depend on conditions at the time of the calibration (Section 5). The effect is largest for UV-B wavelengths (specifically the 305, 313, and 320 nm channels of GUVs) where the solar spectrum increases rapidly because of the strong wavelength dependence of absorption by ozone in the atmosphere. For this reason, Seckmeyer et al. (2010) recommend that the calibration *factor* should be replaced by a calibration *function*, which depends on SZA and TOC. Calibration certificates of GUV instruments provided by BSI typically only provide a calibration factor, but the dependence of this factor on SZA is discussed in Section 5, and these data can be provided upon request.

- **Approach 2 – Response-weighted irradiance**
The objective of Approach 2 is to apply a calibration factor to each channel of the instrument such that the calibrated measurement of a given channel is "response-weighted-irradiance." This quantity is defined as the wavelength integral of the product of spectral irradiance of the source (e.g., the Sun) and spectral response function of the channel (Section 3). If measurements from a spectroradiometer are weighted with the spectral response functions of the collocated filter instrument to be calibrated, the resulting response-weighted-irradiance will be identical with the calibrated measurement of the filter instrument.

The advantage of this calibration approach is that the calibration factor is independent of the radiation source. When measuring solar radiation, the factor does not depend on SZA and TOC. If the calibration factor was established with a standard lamp, it can be applied to solar measurements without corrections. The disadvantage of the approach is that the quantity measured — response-weighted irradiance — is instrument dependent. Comparing the results of different instruments is therefore difficult. However, standardized data products such as the UV Index can be calculated with good accuracy from calibrated values without the need of considering the atmospheric conditions during the time of the measurement (Section 6).

3. IMPLEMENTATION OF CALIBRATIONS AT BSI

The calibration of a GUV radiometer at BSI is executed by exposing the instrument to a light source (either the Sun or a calibration standard), measuring the resulting net signals for each channel (provided in either amps or volts), and comparing this measurement with the physical quantity of interest.

3.1 Implementation using Approach 1

For lamp-based calibrations using Approach 1, the resulting calibration factors for each channel (referred to as "responsivities" in the following) are calculated via:

$$R_{L,i} = \frac{V_{L,i}}{E_L(\lambda_i)} = \frac{(V_{L,i,L} - V_{L,i,D})}{E_L(\lambda_i)}, \quad (1)$$

where $R_{L,i}$ is the responsivity of channel i, $V_{L,i,L}$ is the signal of GUV channel i when exposed to the lamp, $V_{L,i,D}$ is the "dark" signal obtained by covering the GUV collector, $V_{L,i}$ is the net signal, and $E_L(\lambda_i)$ is the spectral irradiance at nominal wavelength λ_i of channel i that is produced by the calibration lamp at the plane of the GUV's collector. The subscript L of each symbol indicates that a lamp was used as the calibration source.

For a solar-based calibration using Approach 1, the GUV is installed next to the SUV-100 (Appendix A.1) and the net signals $V_{S,i}$ of each channel of the GUV is regressed against global spectral irradiance $E_S(\lambda_i)$ measured by the SUV-100 at nominal wavelength λ_i. The slope of the regression is the responsivity $R_{S,i}$ where the subscript S indicates that the instrument is calibrated against the Sun. Note that data points of a scatter plot of $V_{S,i}$ versus $E_S(\lambda_i)$ do not exactly follow a straight line. The regression result is therefore only an approximation and the equation $V_{S,i} = R_{S,i} \times E_S(\lambda_i)$ is not exact. Typically 3 to 5 days of synchronous measurements are performed and used in the regression.

3.2 Implementation using Approach 2

Calibration Approach 2 requires that the spectral response functions of all GUV channels are known. The method to derive these functions is described in Appendix A.2.

Calibrations using Approach 2 take advantage of the fact that the net-signal V_i of a GUV radiometer is proportional to the source spectrum $E(\lambda)$ weighted with the response functions $r_i(\lambda)$ (Seckmeyer et al., 2010):

$$V_i = \gamma_i \times \int E(\lambda) r_i(\lambda) d\lambda\,, \qquad (2)$$

where γ_i is the proportionality constant for channel i. This constant is independent of the source spectrum because Eq. (2) is just an arithmetic description of the physical weighting done by the instrument. Hence, γ_i could be determined with a lamp or a solar spectrum. GUVs are designed to measure the solar spectrum. Because even small errors in $r_i(\lambda)$ can lead to significant errors in γ_i when using lamp spectra (Bernhard et al. 2005), it is more accurate to use solar data. In our implementation, we use spectra of global irradiance $E_S(\lambda)$ measured by the SUV-100. These spectra are first weighted with the spectral response function $r_i(\lambda)$, resulting in the response-weighted irradiance $\hat{E}_{S,i}$:

$$\hat{E}_{S,i} = \int E_S(\lambda) r_i(\lambda) d\lambda\,. \qquad (3)$$

In a second step, measurements of the net signal obtained during solar calibrations, $V_{S,i}$, are regressed against $\hat{E}_{S,i}$. The slope of the regression is the responsivity, denoted $\hat{R}_{S,i}$. If measurements of spectral response functions $r_i(\lambda)$ were without error, the equation $V_{S,i} = \hat{R}_{S,i} \times \hat{E}_{S,i}$ would be exact for any solar spectrum $E_S(\lambda)$, regardless of SZA or other observing conditions. In addition, points of a scatter plot of $V_{S,i}$ versus $\hat{E}_{S,i}$ would be on a straight line, and $\hat{R}_{S,i}$ would equal γ_i.

Once a responsivity is determined with one of the three methods described above, solar measurements of the GUV are calibrated by dividing with this responsivity. For example, the global spectral irradiance $E_S^*(\lambda_i)$ obtained from solar-based calibrations using Approach 1 is:

$$E_S^*(\lambda_i) = \frac{V_{S,i}}{R_{S,i}}\,. \qquad (4)$$

The asterisk (*) of $E_S^*(\lambda_i)$ indicates the calibrated measurement result, which may be different from the true spectral irradiance $E_S(\lambda_i)$, as discussed in more detail in Section 5.

4. DIFFERENCE OF SOLAR- AND LAMP-BASED RESPONSIVITIES DERIVED WITH APPROACH 1.

To understand the difference between responsivities established with Approach 1 using either the Sun or a lamp as a light source, it is helpful to compare the source spectra with the spectral response function of a GUV radiometer. Accordingly, Fig. 1 compares two solar spectra calculated with a radiative transfer model (Mayer and Kylling, 1995) plus the spectrum of an FEL calibration lamp, with the spectral response functions $r_i(\lambda)$ of a GUV radiometer. One of the most remarkable features of Fig. 1 is the rapid change of the solar spectral irradiance between 290 and 320 nm, which is caused ozone absorption in the atmosphere. In comparison, the increase of the lamp's spectral irradiance (shown in red) is much gentler.

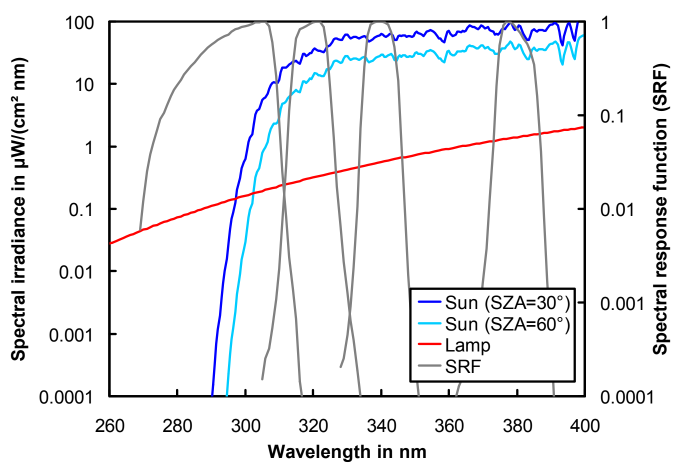

Fig. 1. Comparison of two solar spectrum calculated for SZAs of 30° and 60°, respectively, plus the spectrum of a FEL calibration standard (left axis), with the normalized spectral response functions of a GUV radiometer (right axis). Note that both y-axes are logarithmic. The channel at 313 nm, which is typically also part of a GUV system, was omitted for clarity.

According to Eq. (2), the signal of a GUV channel is proportional to the source spectrum weighted with the spectral response function of that channel. It is therefore instructive to multiply the three spectra shown in Fig. 1 with the GUV's response functions. The resulting "weighted spectra" (i.e., the product $E(\lambda) \times r_i(\lambda)$) are shown in Fig. 2 for the 305, 340, and 380 nm channels. (Results of the 313 and 320 nm channels were omitted for clarity.) Fig. 3 show weighted spectra for the 305 nm channel only.

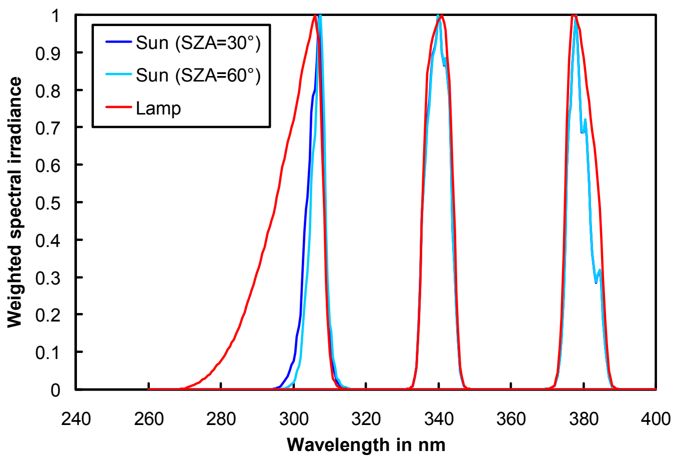

Fig. 2. Weighted spectra, derived by multiplying the two solar spectra and the lamp spectrum of Fig. 1 with the GUV's spectral response functions for 305, 340, and 380 nm. All data were normalized to 1 at their maximum.

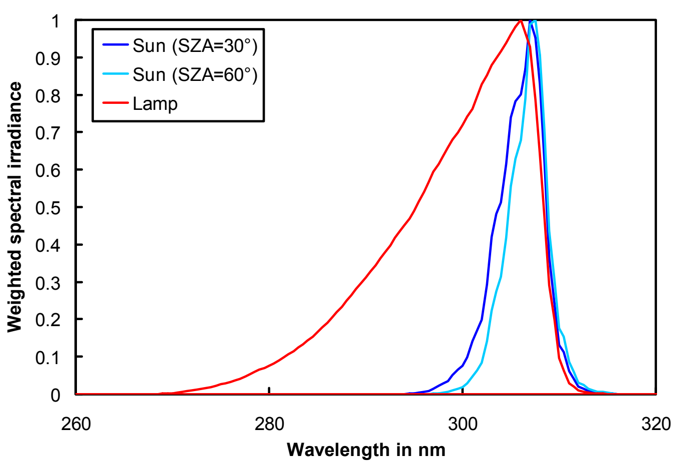

Fig. 3. Same as Fig. 2 but for 305 nm channel only.

As can be seen from Fig. 3, the areas below the blue lines pertaining to the two solar spectra are much smaller than the area below the red line of the lamp spectrum. Wavelengths below 295 nm do not contribute to the signal of the GUV when the instrument is exposed to the Sun but make up a large contribution to the GUV signal when measuring a lamp. The integral $\int E(\lambda) r_i(\lambda) d\lambda$, which is a measure of the area below the weighted spectra, is therefore much smaller for the solar spectra compared to the lamp spectrum. According to Eq. (2), this area is directly related to the signal measured by the GUV. The signal $V_{S,i}$ when measuring the Sun is therefore disproportionally small compared to the signal $V_{L,i}$ when measuring a lamp.

By inserting Eq. (2) into Eq. (1), we can calculate the lamp-based responsivity using Approach 1:

$$R_{L,i} = \frac{\gamma_i \times \int E_L(\lambda) r_i(\lambda) d\lambda}{E_L(\lambda_i)}, \tag{5}$$

A similar equation can be constructed for a solar based calibration using one of the solar spectra shown in Fig. 1:

$$R_{S,i} = \frac{\gamma_i \times \int E_S(\lambda) r_i(\lambda) d\lambda}{E_S(\lambda_i)}, \tag{6}$$

By dividing Eq. (6) with Eq. (5), the ratio of solar- and lamp-based responsivities can now be calculated:

$$\frac{R_{S,i}}{R_{L,i}} = \frac{\int E_S(\lambda) r_i(\lambda) d\lambda}{\int E_L(\lambda) r_i(\lambda) d\lambda} \frac{E_L(\lambda_i)}{E_S(\lambda_i)}, \tag{7}$$

As discussed above, $\int E_S(\lambda) r_i(\lambda) d\lambda$ is much smaller than $\int E_L(\lambda) r_i(\lambda) d\lambda$ for the channel at 305 nm. The ratio of solar- and lamp-based responsivities, $R_{S,i} / R_{L,i}$, is therefore smaller than one. For the channels at 340 and 380 nm, the weighted spectra shown in Fig. 2 are rather similar and it can therefore be expected that the ratio of $R_{S,i} / R_{L,i}$ is close to unity for these channels. For the GUV instrument used as an example in Fig. 1, $R_{S,i} / R_{L,i}$ is 0.487 for the solar spectrum modeled for SZA=30°. These results are consistent with results of the first published systematic analysis of solar- and lamp-based calibrations (Booth et al., 1994).

All GUV radiometers are routinely calibrated using the Sun and a lamp as described in Section 3. Fig. 4 provides examples of ratios $R_{S,i} / R_{L,i}$. The blue line indicates the average ratio calculated from solar- and lamp-based responsivities of 25 instruments. The associated error bars specify the twofold standard deviation of the individual ratios. The red line is the ratio calculate for the instrument used as an example above. For that instrument, the measured ratio at 305 nm is 0.471, which is in good agreement with the ratio of 0.487 calculated theoretically.

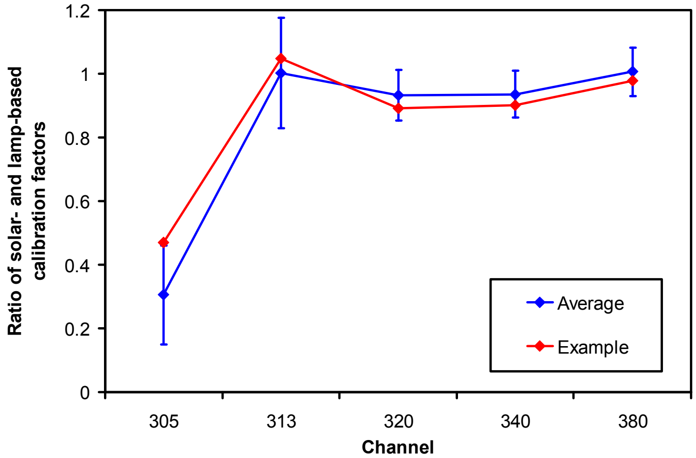

Fig. 4. Ratio of solar-and lamp-based responsivities. The Average refers to the average ratio calculated from solar- and lamp-based responsivities of 25 instruments. The error bar indicates the twofold standard deviation of the individual ratios. The red line is the ratio calculate for the instrument used as an example in the text.

The variation of these ratio between instruments (as expressed by the error bars in Fig. 4) has several reasons, including variations in the spectral response functions from instrument to instrument, and to a lesser extent uncertainties in solar and lamp calibrations.

Fig. 4 also highlights the fact that differences between solar- and lamp-based calibrations are largest for the 305 nm channel, exceeding sometimes 80%. At longer wavelengths, difference are typically smaller than 10%, but may reach up to 20% for some instruments. If a GUV radiometer is used for solar measurements, it is very important to use the solar-based responsivity for the 305 nm channel. For the other channels, use of the lamp-based responsivities gives typically reasonably accurate results also.

BSI has historically provided solar- and lamp-based responsivities for every instrument. This led to some confusion. The responsivities listed in more recent calibration certificates shipped with instruments are based on a solar calibration for the 305 and 313 channels and a lamp calibration for all other channels. However, a complete set of responsivities can be provided upon request.

5. SYSTEMATIC ERRORS IN CALIBRATED SOLAR DATA AND THEIR CORRECTION

As already mentioned in Section 2, data of global spectral irradiance $E_S^*(\lambda_i)$ that are derived from GUV measurements with Eq. (4) may deviate from the true spectral irradiance $E_S(\lambda_i)$ to some degree. In contrast, response-weighted-irradiance data derived from the same GUV raw data by applying Approach 2 agree well with $\hat{E}_{S,i}$. This observation is illustrated by comparing calibrated GUV data to SUV-100 data. The latter are assumed to represent the truth.

Fig. 5 shows the ratios of calibrated GUV data and SUV-100 using either Approach 1 (solid blue markers) or Approach 2 (solid red markers). GUV data obtained with Approach 1 agree to within ±5% with SUV-100 data for SZAs smaller than about 50°. For larger SZAs, GUV overestimate the spectral irradiance. The maximum overestimation of about 50% occurs at about SZA=75°. In contrast, GUV data calibrated with Approach 2 agree to within ±7% for SZAs up to 88°. The GUV instrument used for this comparison is the same that was featured in Section 4. Because spectral response functions vary from instrument to instrument, the pattern shown in Fig. 5 is not the same for all GUV radiometers.

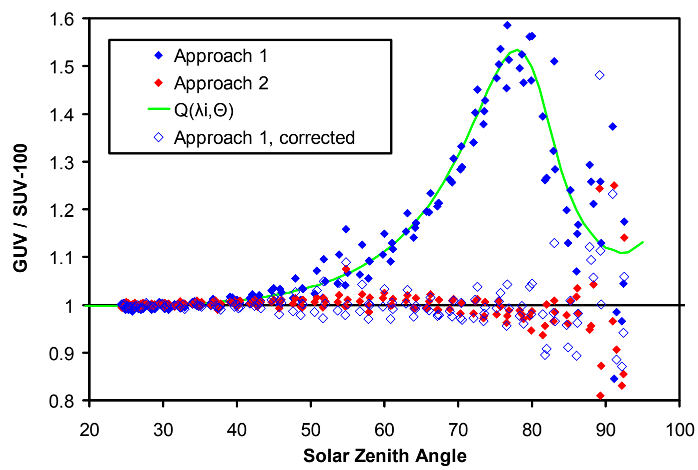

Fig. 5. Ratio of calibrated GUV and SUV-100 data. GUV data were calibrated with the solar-based Approach 1 (solid blue markers) and Approach 2 (solid red markers). The green line is the function $Q_S(\lambda_i,\theta)$, calculated with Eq. (8). Open blue markers indicate the ratio of GUV and SUV-100 data calibrated with Approach 1 and corrected by dividing with $Q_S(\lambda_i,\theta)$. Data were collected in San Diego between 31 August and 2 September 2014. The total ozone column at this time varied between 283 and 296 DU.

The ratio of measured and true spectral irradiance is denoted $Q_S(\lambda_i,\theta)$ in the following ($Q_S(\lambda_i,\theta) \equiv E_S^*(\lambda_i,\theta)$ / $E_S(\lambda_i,\theta)$ where θ indicates the SZA). The dependence of $Q_S(\lambda_i,\theta)$ on SZA indicated in Fig. 5 has two reasons: first, the SUV-100 radiometer has a bandwidth of 1 nm while that of the GUV is considerably larger. Second, as the SZA changes, the weighted spectrum also changes (compare the light and dark blue lines in Fig. 3).

The ratio $Q_S(\lambda_i, \theta)$ can be calculated as:

$$Q_S(\lambda_i, \theta) = \frac{\int E_S(\lambda, \theta_R) r_i(\lambda) d\lambda}{\int E_R(\lambda, \theta) r_i(\lambda) d\lambda} \frac{E_R(\lambda_i, \theta)}{E_S(\lambda_i, \theta_R)}, \qquad (8)$$

where $E_R(\lambda, \theta_R)$ is the solar spectral irradiance at θ_R (i.e., the reference SZA), and $E_R(\lambda_i, \theta_R)$ is the spectral irradiance at the nominal wavelength λ_i and at θ_R. Note that Eq. (8) is of the same type as the ratio of solar- and lamp-based calibrations discussed in Section 4 and expressed in Eq. (7). Note also that $Q_S(\lambda_i, \theta)$ is equivalent to the correction function $K_i^{(2)}$ defined by Seckmeyer et al. (2010). $Q_S(\lambda_i, \theta)$ can be readily calculated from modeled solar spectra. A list of suitable radiative transfer models is provided in Appendix 2 of Seckmeyer et al. (2010).

The green line in Fig. 5 indicates $Q_S(\lambda_i, \theta)$ and was calculated with Eq. (8) for θ_R=30° using spectra modeled with the UVSPEC radiative transfer model (Mayer and Kylling, 1995). The total ozone column was set to 290 DU. The reference SZA of θ_R=30° was chosen because of the excellent agreement of GUV and SUV-100 data at this SZA. GUV data calibrated with Approach 1 were divided by $Q_S(\lambda_i, \theta)$ to correct for the SZA effect. Results (open blue markers in Fig. 5) agree with SUV-100 data to within ±5% up to a SZA of 80°, with the exception of one outlier caused by variability introduced by clouds.

It should be noted that $Q_S(\lambda_i, \theta)$ does not only depend on SZA but also on TOC, albeit to a lesser extent. The TOC-dependence can be easily taken into consideration by including TOC in Eq. (8). This requires that model spectra are calculated for different TOCs and SZAs. Seckmeyer et al. (2010) recommend that both SZA and TOC are taken into account.

As an alternative to the correction method described above, the SZA-dependence of $Q_S(\lambda_i, \theta)$ can also be parameterized by fitting a function to the uncorrected ratio of $E_S^*(\lambda_i)$ and $E_S(\lambda_i)$. This method should only be applied if the TOC during the calibration of the instrument is similar to within about 50 DU with that at the deployment site of the instrument. If variations in ozone are larger, the model-based method (i.e., Eq. (8)) is preferred (Seckmeyer et al., 2010).

A SZA-effect of similar magnitude as that indicated in Fig. 5 for the 305 channel is typically also observed for the 313 nm channels. For the 320 nm channel, the SZA-dependence is smaller than 10% for SZAs up to 85°, and for channels with longer wavelengths, the ratio of GUV and SUV data has virtually no SZA dependence.

As noted earlier, BSI provides spectral response functions of GUV instruments only if requested by a customer. Without these functions, the correction method discussed above cannot be implemented. For customers that require accurate measurements of spectral irradiance also at larger SZA, we recommend to request a spectral characterization when ordering the instrument. As an alternative, the ratios of $E_S^*(\lambda_i)$ and $E_S(\lambda_i)$ (blue markers in Fig. 5) for constructing a correction function can also be provided. As noted earlier, this approach is not recommended if TOCs observed during the calibration and at the deployment site differ.

6. CALCULATION OF DATA PRODUCTS

Most GUV radiometers are used to measure biologically effective irradiance (see Glossary). The most important biological quantity is the UV Index (UVI), which is a measure of the ability of UV radiation to cause erythema (sunburn) in human skin (WHO 2002). The wavelength dependence of the erythemal response has been standardized by the International Commission on Illumination (CIE) in 1987 (McKinlay and Diffey, 1987a; 1987b). Although the function defined in this norm has been updated in 1998 (CIE, 1998), the original norm is still widely being used and the UV Index discussed below is based on CIE (1987b)[2].

The UVI and other data products (e.g., UV-B, UV-A) can be calculated from GUV data that may be calibrated either with Approach 1 or 2. Both methods are used by BSI and are discussed below.

6.1 Calculation of data products with Approach 1.

The calculation of a data product D (e.g., the UVI) from measurements of a multi-filter instrument that was calibrated with Approach 1 is typically implemented via a linear

[2] For SZAs < 40°, UV Indices calculated according to CIE (1987b) are less than 0.5% smaller than those calculated according to CIE (1998). For SZAs < 65°, the difference reamains less than 1%, but increases to 2% at SZA=85° (Webb et al., 2011).

combination (e.g., Dahlback, 1996; Bernhard, 2005; Seckmeyer et al., 2010):

$$D = \sum_i a_i E^*(\lambda_i)\,, \tag{9}$$

where a_i are coefficients and $E^*(\lambda_i)$ are spectral irradiances measured by the instrument at the nominal wavelength λ_i. The coefficients a_i are determined with a multiple linear regression.

UV Indices calculated with this method may deviate from the true UVI and a correction function depending on SZA is sometimes being applied (e.g., Dahlback, 1996). The following analysis shows that this is typically not necessary.

BSI has historically recommended to use one of the following parameterizations[3] to calculate the UVI:

$$UVI = 0.8911E^*(305) + 0.0818E^*(320) + 0.007751E^*(340) \tag{10}$$

$$UVI = 0.8058E^*(305) + 0.0887E^*(313) + 0.0324E^*(320) + 0.0131E^*(340) \tag{11}$$

where the spectral irradiances $E^*(\lambda_i)$ have to be expressed in units of µW/(cm^2 nm).

The accuracy of these parameterizations was re-evaluated by calculating the UVI according to Eqs. (10) and (11) using spectral irradiance measured by the SUV-100 at 305, 313, 320, and 340 nm, and comparing these data with the UVI calculated from the SUV-100's full resolution spectra. Fig. 6 shows the results for the 3-parameter parameterization (Eq. (10)). The slope of the regression to the data points is 1.0030, indicating that the parameterization is able to reproduced the true UVI with only a small bias of 0.3%. For 98% of all data points, the difference between parameterized and measured UVI values (orange markers in Fig. 6) is smaller than ±0.2 UVI units. The 4-parameter parameterization (Eq. (11)) does not produce a better correlation.

Fig. 6 does not include GUV data; it is solely based on measurements of the SUV-100 and the spectral irradiances used in Eq. (10) are therefore not affected by systematic errors that influence GUV data at large SZAs (e.g., Fig. 5).

The analysis was repeated by calibrating a GUV against SUV-100 data using Approach 1; applying Eq. (4) to calculate $E_S^*(305)$, $E_S^*(320)$, and $E_S^*(340)$; parameterizing the UVI from these measurements by applying Eq. (10); and finally correlating the result with UVI values derived from full-resolution spectra of the SUV-100.

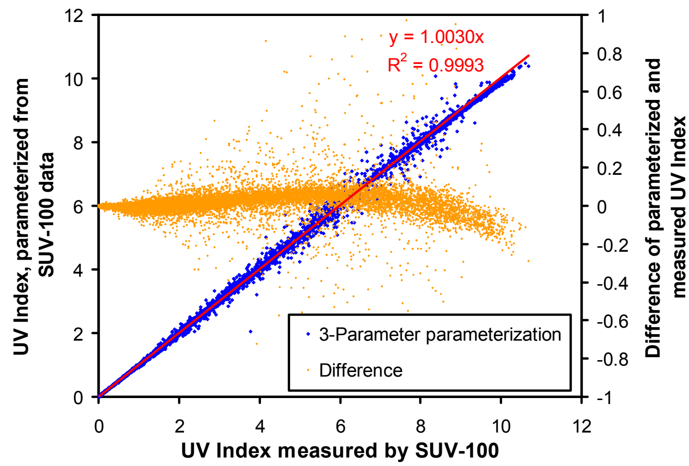

Fig. 6. Scatter plot of UV Index parameterized with Eq. (10) from spectral irradiance at 305, 320, and 340 nm measured by the SUV-100 versus the UV Index calculated from full-resolution SUV-100 spectra (blue markers, left axis). The regression line, slope, and coefficient of determination are indicated in red. Shown in orange is the difference of parameterized and measured UVI (right axis). Data were measured in San Diego between August 2003 and October 2004 (19,621 data points).

Results are shown in Fig. 7, and these are very similar to those of Fig. 6. This suggests that the UVI can be calculated from GUV data with an accuracy comparable to that of spectral SUV-100 data. (The fraction of parameterized data that agree with measured UVI values to within ±0.2 UVI units is 0.97%, which is only slight lower than the fraction pertaining to Fig. 6). This result is important considering that measurements of a GUV's 305 channel can deviate considerably from the true spectral irradiance at larger SZAs (Fig. 5). The explanation of this perhaps surprising finding is that the spectral irradiance at 305 nm contributes less and less to the UVI than the spectral irradiance at 320 and 340 nm as the SZA gets larger. Hence, systematic errors in $E_S^*(305)$ are of lesser importance at large SZAs.

The analysis described above was repeated with data from the 31 August to 2 September 2014 period discussed in

[3] http://www.biospherical.com/index.php?option=com_fss&view=faq&Itemid=116&catid=1&faqid=18

Section 5 with similar results. This confirms that the 3-parameter fit of Eq. (10) is robust.

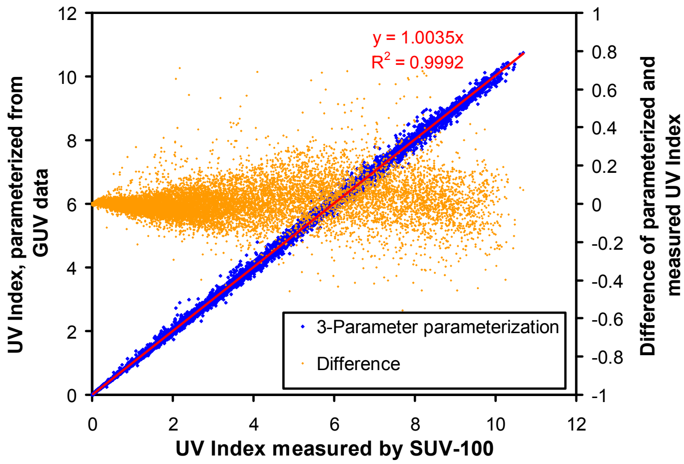

Fig. 7. Similar to Fig. 6, but parameterized dataset is based on GUV data.

As noted in Section 4. the standard set of responsivities distributed with GUV instruments are based on a solar calibration for the 305 and 313 channels and a lamp calibration for all other channels. Since solar-based responsivities at 320 and 340 nm tend to be smaller than lambased ones by about 7% (Fig. 4), the solar-based responsivities used above were scaled accordingly and the UVI was recalculated. The UVI with the modified set of coefficients is smaller by about 2.5%. Hence, the use of lamp-based coefficients for the two channels leads to a systematic bias, but this bias is smaller than the uncertainty of SUV-100 of about 6% (2σ) against which GUVs are calibrated.

Parameterizations to calculate UV-B and UV-A irradiance were also developed, resulting in equations similar to Eqs. (10) and (11). We note that UV-B and UV-A are not unambiguously defined. Some research communities define UV-B as the integral of 280–315 nm (which is more appropriate), some use 280–320 nm. The choice of the upper wavelength makes a big difference because of the dramatic change of the solar spectrum at Earth's surface in this wavelength range (Fig. 1). Likewise, UV-A is sometimes defined as 315–400 nm and sometimes as 320–400 nm. Here the difference is small as the wavelength interval of 315–320 nm contributes only very little. Box 1 provides parameterizations for the four wavelength ranges.

Box 1. Coefficients for calculating UV-B and UV-A irradiance.

UV-B (290–315 nm) = 8.91 $E(305)$ + 5.13 $E(313)$

UV-B (290–320 nm) = -1.373 $E(305)$ + 14.6 $E(313)$

UV-A (315–400 nm) = 32.57 $E(340)$ + 42.86 $E(380)$

UV-A (320–400 nm) = 30.27 $E(340)$ + 43.15 $E(380)$

Note that spectral irradiances have to be provided in units of μW/(cm^2 nm).

6.2 Calculation of data products with Approach 2.

The calculation of a data product from GUV measurements that were calibrated with Approach 2 is implemented using a method originally proposed by Dahlback (1996). In brief, data product D is approximated by a linear combination of $V_{S,i}$:

$$D = \sum_i b_i V_{S,i} \,, \tag{12}$$

The coefficients b_i are calculated by solving a system of linear equations (see also Eq. (7) of Dahlback (1996)):

$$\sum_i \left(b_i \hat{R}_{S,i} \int_0^\infty r_i(\lambda) E_{M_j}(\lambda) d\lambda \right) = \int_0^\infty A(\lambda) E_{M_j}(\lambda) d\lambda \,, \tag{13}$$

where $A(\lambda)$ is the “action spectrum” (see Glossary) of the biological effect under consideration, and $E_{M_j}(\lambda)$ are model spectra calculated for different SZAs and ozone columns. These spectra are required to quantify the relative spectral difference between the response functions and the action spectrum, and are calculate at BSI with the UVSPEC model (Mayer and Kylling, 1995). Note that the responsivity $\hat{R}_{S,i}$ used in Eq. (13) has to be established with Approach 2 (Section 3.2). The number of GUV channels i used in Eq. (13), may range between 1 and 5, depending on the action spectrum used, and the number of model spectra required for the inversion has to match this number. Additional information on BSI's implementation of the method is provided by Bernhard et al. (2005).

The method has been implemented at BSI to produce a large number of data products for GUVs that are part of the NSF UV Monitoring Network and follow-on projects (http://uv.biospherical.com/). A list of data products that that are currently being produced can be found at http://uv.biospherical.com/login/GUV/description-GUV-data-products.html and additional references are also provided by Bernhard et al. (2005).

Sets of coefficients b_i to produce these data products according to Eq. (12) can be shipped with any GUV instrument whose spectral response functions have been characterized. Please contact BSI if you are interested in this service.

6.3 Calculation of total ozone column.

The calculation of TOC from GUV measurements is implemented with lookup tables, which relate total column ozone to SZA and the ratio of GUV measurements at 305 and 340 nm. The retrieval method is similar to the method described by Stamnes et al. (1991). The method requires that the spectral response functions for the two channels have been characterized. More information on BSI's implementation is provided by Bernhard et al. (2005).

APPENDICES

A.1 The SUV-100 spectroradiometer

The SUV-100 is a scanning spectroradiometer manufactured by BSI and permanently installed on the roof platform of BSI. The instrument measures global spectral irradiance between 280 and 600 nm with a spectral resolution (bandwidth) of 1 nm. The system is fully-automated and uses a temperature-stabilized, scanning double-monochromator coupled to a photomultiplier tube (PMT) detector. A heated diffuser made of PTFE serves as irradiance collector. Lamps for automated wavelength and intensity stability checks are integrated in the system. The system is calibrated every two weeks with irradiance standard lamps, which are mounted above the irradiance collector in a specially designed lamp housing. The scale of spectral irradiance of these standard lamps is traceable to the scale of spectral irradiance maintained by the U.S. National Institute of Standards and Technology, and frequently verified. Measurements have an uncertainty of about 6% (2σ). Before SUV-100 data are used to calibrate GUV radiometers, they are corrected for wavelength shifts and the cosine error of the PTFE diffuser. More information on the SUV-100 can be found at:
http://uv.biospherical.com/report_0001/CHAPTER2.PDF.

A.2 Measurement of spectral response functions

The spectral response functions of GUV radiometers are characterized with BSI's Spectral Response Tester (SRT). The apparatus consists of a 1000-Watt xenon arc lamp and a grating double monochromator with prism predisperser, designed and built by BSI. The two single monochromators that make up the double monochromator are stacked vertically and share a common shaft to which the gratings are mounted. This design ensures that the two single monochromators are always synchronized. Each of the two monochromators is equipped with three diffraction gratings (Table 1). UV channels of GUV radiometers are characterized with Grating 1.

The intensity of radiation exiting the monochromator is characterized as a function of the monochromator's wavelength setting with photodiodes that have a responsivity calibration traceable to NIST. The current produced by these reference detectors is measured with a picoammeter.

For determining the wavelength mapping of the monochromator, a mercury-argon (HgAr) discharge lamp is mounted in front of the entrance slit of the monochromator. Table 1 gives an overview of the specifications of the SRT.

Table 1. Specifications of the Spectral Response Tester.

Monochromator	
Type	Czerny-Turner double monochromator in additive configuration with prism predisperser
Focal length	500 mm
Focal ratio	f/5
Grating configuration	Grating 1: 2,400 grooves/mm Grating 2: 1,200 grooves/mm Grating 3: 300 grooves/mm
Dispersion	Grating 1: 0.35 nm/mm Grating 2: 0.69 nm/mm Grating 3: 2.8 nm/mm
Wavelength range	Grating 1: 200 - 600 nm Grating 2: 600 - 1,100 nm Grating 3: 1,100 - 2,000 nm
Wavelength accuracy	Grating 1: ±0.2 nm Grating 2: ±0.4 nm Grating 3: ±1.6 nm
Light sources	
Illumination	1000-Watt xenon arc lamp (Model SP66926-3477 from Thermo Oriel)
Wavelength standard	HgAr low pressure Pen ray discharge lamp
Detectors	
UV and visible	Model 818-UV from Newport
Infrared	Model 818-IG from Newport

For characterizing their spectral response functions the test GUV is placed directly behind the monochromator's exit slit with the beam exiting the monochromator centered on the diffuser of the test systems. The spectral response of a channel of a test system is determined by comparing the output signal of that channel against the signal of the reference silicon photodiode as a function of wavelength. The resulting functions are inherently smoothed due to the finite bandwidth of the monochromator (Table 1). This smoothing effect is corrected with a deconvolution algorithm described by Bernhard et al. (2005). Spectral response functions $r_i(\lambda)$ are normalized to one at their maximum. These functions are shown in Fig. 8 for a GUVis-3511 radiometer equipped with 19 channels.

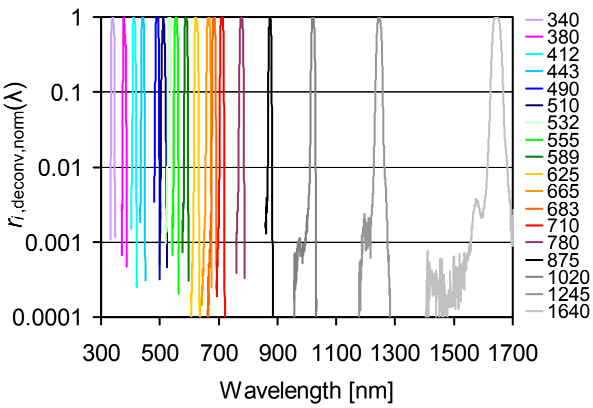

Fig. 8. Normalized spectral response functions of a GUVis-3511 radiometer equipped with 19 channels. The legend indicates the nominal wavelengths of each channel.

The wavelength accuracy of the spectral tester is about 0.2 nm when using Grating 1 (Table 1). According to Appendix C.1 of Seckmeyer et al. (2010), a wavelength shift of 0.03 nm at the nominal wavelength of 305 nm for a channel with a bandwidth of 10.0 nm full width of half maximum can lead to errors in the response weighted irradiance $\hat{E}_{S,305}$ of up to 2%. (Interestingly, the error is almost independent of bandwidth, so reducing the spectral bandpass of GUV channels would not reduce the error.) For applications where the highest accuracy achievable is required, an iterative method is applied to reduce the wavelength uncertainty of $r_i(\lambda)$ to about 0.05 nm: first, GUVs are calibrated with Approach 2 (Section 3.1) and the ratio of GUV and SUV-100 data is calculated. If there is a significant wavelength error, the ratio would depend on SZA as discussed in Section 5. If that is the case, the measured spectral response functions are shifted in wavelength, and the procedure is repeated until the ratio of GUV and SUV measurements becomes independent of SZA. The process is time intensive and therefore offered on request only.

A.3 Glossary

<u>Action spectrum</u>

See biologically effective irradiance.

<u>Biologically effective irradiance; biological weighting function; action spectrum</u>

A biological weighting function or action spectra $A(\lambda)$ describe the wavelength dependence of effects introduced by electromagnetic radiation on biological matter. Depending on the effect and the involved organism different biological weighting functions are used. The biologically effective irradiance D is calculated by multiplying global spectral irradiance $E_S(\lambda)$ with the action spectrum $A(\lambda)$ and integrating over wavelength λ:

$$D = \int E_S(\lambda)A(\lambda)d\lambda\ , \tag{14}$$

<u>Global spectral irradiance</u>

Global spectral irradiance $E_S(\lambda)$ is defined as radiant energy arriving per time interval, per wavelength interval, and per area on a horizontal surface from all parts of the sky above the horizontal, including the disc of the sun itself.

<u>Response-weighted-irradiance</u>

Response-weighted irradiance $\hat{E}_i$ is defined as the integral of the product of spectral irradiance $E(\lambda)$ and the spectral response function $r_i(\lambda)$ of channel i from a multi-filter radiometer:

$$\hat{E}_i = \int E(\lambda)r_i(\lambda)d\lambda\ . \tag{15}$$

<u>Spectral response function</u>

The spectral response function $r_i(\lambda)$ of a specific channel i of a filter radiometer, is the ratio of the signal $dV(\lambda)$ to the spectral irradiance $dE(\lambda)$ at the place of the radiometer's collector, as a function of wavelength λ:

$$r_i(\lambda)=\frac{dV(\lambda)}{dE(\lambda)}\ . \tag{16}$$

Spectral response functions are typically normalized to one at their maximum.

<u>Total ozone column</u>

Total ozone column (TOC) is the height of a hypothetical layer which would result if all ozone molecules in a vertical column above the Earth's surface were brought to standard pressure (1013.25 hPa) and temperature (273.15 K). The total ozone column is usually reported in “Dobson units” (DU). The global average ozone amount is close to 300 DU, which corresponds to a layer of 3 mm thickness.

References

Bernhard, G., C. R. Booth, and J. C. Ehramjian. (2005). Real-time ultraviolet and column ozone from multichannel ultraviolet radiometers deployed in the National Science Foundation's ultraviolet monitoring network. *Optical Engineering*, **44**(4), 041011-1 - 041011-12.

Booth, C.R., T. Mestechkina, and J.H. Morrow. (1994). Errors in the reporting of solar spectral irradiance using moderate bandwidth radiometers: an experimental investigation. in: Ocean Optics XII, *Proc. SPIE Int. Soc. Opt. Eng.*, **2258**, 654-663.

BSI (2012). *Application Note: Light Quantities, Units, and Conversion Factors*, Biospherical Instruments, AN-2012-0001-Rev1, 6 pp. available from the Support section at www.biospherical.com.

CIE (Commission Internationale de l'Éclairage) (1998). *Erythema Reference Action Spectrum and Standard Erythema Dose*. CIE S007E-1998. CIE Central Bureau, Vienna, Austria.

Mayer, B., and A. Kylling. (2005). Technical Note: The libRadtran software package for radiative transfer calculations: Description and examples of use. *Atmos. Chem. Phys.*, **5**:1855-1877.

McKinlay, A. F. and B. L. Diffey (1987a): A reference action spectrum for ultraviolet induced erythema in human skin. In *Human Exposure to Ultraviolet Radiation: Risks and Regulations* (Edited by W. F. Passchier and B. F. Bosnjakovic), pp. 83–87, Elsevier, Amsterdam, The Netherlands.

McKinlay, A. F. and B. L. Diffey (1987b): A reference action spectrum for ultraviolet induced erythemal in human skin. *CIE J.*, **6**(1), 17–22.

Seckmeyer, A. Bais, G. Bernhard, M. Blumthaler, B. Johnsen, K. Lantz, and R. McKenzie with contributions from S. Diaz, P. Disterhoft, L. Jalkanen, A. Kazantzidis, P. Kiedron, B. Petkov, C. Sinclair, and C. Wilson. (2010). *Instruments to Measure Solar Ultraviolet Radiation. Part 3: Multi-channel filter instruments*, WMO Global Atmospheric Watch Report No. 190, WMO/TD-No. 1537, World Meteorological Organization, Geneva, Switzerland.

Stamnes, K., J. Slusser, and M. Bowen (1991): Derivation of total ozone abundance and cloud effects from spectral irradiance measurements, *Appl. Opt.*, **30**(30), 4418-4426.

Webb, A. R., Slaper, H., Koepke, P., & Schmalwieser, A. W. (2011). Know your standard: clarifying the CIE erythema action spectrum. *Photochem. Photobiol.*, **87**(2), 483-486.

WHO (2002): *Global Solar UV Index: A Practical Guide*, 28 pp., published by World Health Organization (WHO), World Meteorological Organization (WMO), United Nations Environment Programme (UNEP), and the International Commission on Non-Ionizing Radiation Protection (ICNIRP), WHO, Geneva, Switzerland, ISBN 9241590076. Available at: http://www.who.int/uv/publications/en/GlobalUVI.pdf.